Quantum Electronics **34** (12) 1163 – 1168 (2004)

NONLINEAR OPTICAL PHENOMENA

PACS numbers: 42.65.Jx; 42.60.Jf
DOI: 10.1070/QE2004v034n12ABEH002730

Specific features of elliptic beam self-focusing

V.P. Kandidov, V.Yu. Fedorov

***Abstract*. Stationary self-focusing of collimated elliptic Gaussian beams is studied numerically. It is shown that the critical self-focusing power increases with increasing the axial ratio of the initial elliptic cross section. Self-focusing is accompanied by oscillations of the beam transverse size caused by the competition between the diffraction-limited divergence and nonlinear compression. As the power of the beam with the axial ratio $a/b \geqslant 3$ increases, aberration self-focusing occurs, at which, after the formation and competition of several intensity maxima in the beam cross section, a global maximum appears at the beam centre, which forms a nonlinear focus. The approximation formula for the self-focusing distance is generalised to elliptic beams.**

Keywords: *self-focusing, elliptic beams, critical power, self-focusing distance, aberration self-focusing, variational-difference scheme.*

1. State of the art of the studies

Laser beams with the elliptic cross section have long attracted the attention of researchers from the point of view of both fundamental studies and applications. At present interest in the problem of self-action of elliptic beams is related to a rapidly developing nonlinear optics of femtosecond laser radiation [1 – 3]. Upon propagation of femtosecond pulses with power exceeding the critical self-focusing power in the medium, extended filaments are formed in which a significant part of the incident radiation energy is concentrated [4, 5]. In the atmosphere, the length of filaments produced by pulses from a Ti : sapphire laser achieves a few hundreds of metres, their diameter is 100 μm, the intensity of the light field in a filament is $\sim 10^{13}$ W cm^{-2}, and the spectrum covers a broad range from 0.5 to 3 μm [6, 7]. A supercontinuum pulse produced during the propagation of high-power laser pulses in air can be used for broadband laser probing and ecological monitoring of the environment [1].

In terawatt pulses, a bunch of filaments is produced, which appear due to a spatial instability of the intense light field in a medium with cubic nonlinearity [8]. The perturbations of the intensity and phase of the light field in the cross section of the pulse, caused by the quality of the laser beam and fluctuations of the refractive index in air, result in the spatial randomisation of the filament bunch [9]. Signals of fluorescence and backscattering from the components of air prove to be irregular, which complicates practical applications of femtosecond laser pulses for laser probing. Therefore, the problem of regularisation of the process of formation of filaments in a terawatt femtosecond pulse is quite urgent.

One can expect that the use of pulses with a special intensity distribution at the output of a laser system will regulate the formation of many filaments during the pulse propagation under real conditions. One of such intensity distributions is inherent in elliptic beams.

The self-focusing of elliptic beams was first studied by the variational method in [10]. Within the framework of the aberration-free approximation, using the stationary Lagrangian for the light field in a medium with cubic nonlinearity, a system of ordinary differential equations was written, which describes the dependences of the field amplitude and semiaxes of the elliptic cross section of the beam on the distance. The critical self-focusing power $P_{\rm cr}^{\rm est}$ for an elliptic beam was analytically estimated from this system of equations as

$$P_{\rm cr}^{\rm est} = 2\,\frac{a^2+b^2}{ab}\,\frac{\pi n_0}{2k^2 n_2}, \qquad (1)$$

where a and b are the semiaxes of the elliptic cross section determined at the e^{-1} level of the intensity profile; k is the wave number; n_0 is the refractive index; and n_2 is the nonlinearity coefficient. The results of the variational analysis and experimental study of the self-focusing of elliptic beams were discussed in review [11]. The numerical simulation of self-focusing of elliptic beams gave a more accurate value of the critical self-focusing power [12].

In 1990s interest in theoretical studies of the self-focusing of elliptic beam was rekindled. In [13], the solutions found by the axial method [14] were analysed within the framework of the aberration-free approximation, in which the transverse distribution of the field remains close to Gaussian [see (2)], and a classification of the propagation regimes of the beam depending on the relation between its parameters was proposed. The aberration-free approximation was used in [15], where a system of equations for the parameters of a Gaussian beam obtained by the variational method [10] was numerically solved. It is stated that the self-channeling regime of an elliptic beam is impossible because at the constant effective radius $[a^2(z)+b^2(z)]^{1/2}$ of the

V.P. Kandidov, V.Yu. Fedorov Department of Physics, M.V. Lomonosov Moscow State University, Vorob'evy gory, 119992 Moscow, Russia

Received 20 April 2004; revision received 23 August 2004
Kvantovaya Elektronika **34** (12) 1163 – 1168 (2004)
Translated by M.N. Sapozhnikov

beam, the undamped oscillations of the lengths of its semiaxes $a(z)$ and $b(z)$ occur during propagation.

The aberration-free approximation used in the axial and variational methods was analysed in detail in [16]. It was shown that this approximation leads to considerable deviations of the obtained solutions from the results of numerical simulation. In the case of strong ellipticity of the initial distribution of the radiation intensity in the beam, rings can be formed in the cross section plane; directly in front of a nonlinear focus, the elliptic beam transforms to a circular beam.

In [17], the critical self-focusing power P_{cr} was numerically determined for beams with weak ellipticity ($a/b < 2.5$), and the empirical formula was obtained for it. It was shown that the collapse of the elliptic beam encompasses not the entire beam, but only a part of its cross section, where an axially symmetric profile, close to the Townes mode [18], is formed directly in front of the nonlinear focus. An increase in the critical self-focusing power for beams with the initial profile different from the Townes mode was explained [19] by the transfer of the pump power outside the collapse region.

In this paper, we studied numerically the stationary self-focusing of elliptic beams in broad ranges of the beam power and the axial ratio of beam cross sections in order to analyse the properties of formation of nonlinear foci in such beams and to obtain approximate expressions for practical calculations of the critical power and self-focusing length of elliptic beams.

2. Formulation of the problem

The distribution of the field amplitude in the cross section of a collimated elliptic beam has the form

$$E(x, y, z = 0) = E_0 \exp\left(-\frac{x^2}{2a^2} - \frac{y^2}{2b^2}\right). \quad (2)$$

In the scalar approximation, the complex amplitude $E(x, y, z)$ in the case of stationary self-focusing is described by the equation

$$2ik\,\frac{\partial E}{\partial z} = \frac{\partial^2 E}{\partial x^2} + \frac{\partial^2 E}{\partial y^2} + \frac{2k^2}{n_0}\,n_2|E|^2 E. \quad (3)$$

The numerical study of the three-dimensional problem (2), (3) of beam self-focusing involves considerable difficulties because the localisation scales of the light field change many times in the beam cross section and strong phase gradients appear. To reproduce adequately such variations in the light field, it is necessary to use a calculation grid with a small step, which results in time consuming calculations. In the case of beams with high ellipticity, the calculations become additionally complicated due to a great difference between the values of a and b in the initial distribution of the light field (2). To overcome these difficulties, we used in this paper the efficient calculation method (see Appendix) employing a nonuniform grid in the beam cross section XY.

The nonuniform grid consists of the axial region with a uniform small step h_0 of the spatial division and of the periphery region, in which the grid step h_m slowly increases as

$$h_{m+1} = h_m(1 + \varepsilon), \quad (4)$$

where ε is the increase parameter, which is much smaller than unity; $m = -N/2, \ldots, 0, \ldots, N/2$ is the step number; and N is the number of steps. We used such a nonuniform grid to study self-focusing because the light-field collapse, which is manifested in the appearance of large spatial gradients of the nonlinear phase shift and in the avalanche increase in the light-field intensity, occurs in the axial region of the beam, where a small division step is needed. At the periphery, where the variations in the intensity and phase of the light field, caused mainly by diffraction, are small, a much larger grid step can be used.

3. Critical self-focusing power

The critical self-focusing power P_{cr} of elliptic beams was determined from a number of numerical experiments performed at different powers P and axial ratios a/b of the initial elliptic cross section. To analyse the dependence of P_{cr} on the ratio a/b, it is convenient to present this dependence in the form

$$P_{cr}(a/b) = R_{cr}(a/b)\,\frac{\pi n_0}{2k^2 n_2}, \quad (5)$$

where $R_{cr}(a/b)$ is the critical nonlinearity parameter. Note that for a circular collimated Gaussian beam, the critical nonlinearity parameter is $R_{cr}(a/b = 1) = 3.77$ [11]; a circular beam with the cross-section intensity distribution coinciding with the Townes mode has the lowest self-focusing power with the nonlinearity parameter $R_{cr}^{Town}(a/b = 1) = 3.72$ [18]. The axial method using aberration-free approximation [14] strongly underestimates the nonlinearity parameter, giving the value $R_{cr}^{parax}(a/b = 1) = 1$ for a circular beam.

Figure 1 shows the dependence of the critical nonlinearity parameter R_{cr} on the axial ratio a/b obtained by numerical simulation. As the axial ratio a/b increases, the critical self-focusing power P_{cr} rises, which is explained by the increasing difference of the elliptic intensity distribution from the Townes mode. The figure also demonstrates this dependence for the nonlinearity parameter R_{cr}^{est} corresponding to the critical power calculated by the variational method within the framework of the aberration-free approximation [10]. One can see that the variational method with

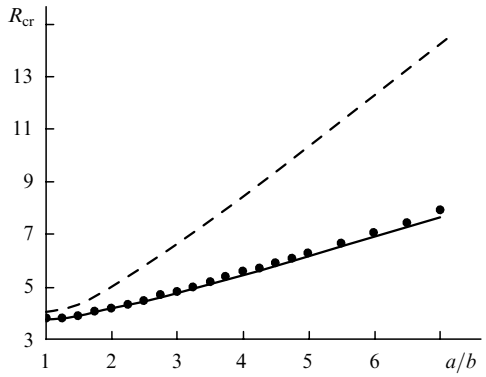

Figure 1. Dependences of the critical nonlinearity parameter R_{cr} on the axial ratio a/b of the initial elliptic cross section of a collimated Gaussian beam: circles are numerical simulation; the dashed curve is the variational estimate R_{cr}^{est} (1); the solid curve is empirical expression (6).

the aberration-free approximation overestimates the critical self-focusing power for an elliptic beam. In this case, as the axial ratio a/b increases, the deviation of the variational estimate of $R_{\rm cr}^{\rm est}$ from $R_{\rm cr}$ calculated numerically increases. The numerical values of the parameter $R_{\rm cr}(a/b)$ are well approximated by the empirical dependence

$$R_{\rm cr}(a/b) \approx \left[0.4\,\frac{a/b + b/a}{2} + 0.6\right] R_{\rm cr}(a/b = 1) \qquad (6)$$

proposed in [17].

4. Oscillations of the beam cross section and the power flux

The self-focusing of Gaussian beams with the elliptic cross section is accompanied by periodic variations in the beam size. For $P > P_{\rm cr}$, oscillations of semiaxes with distance occur against the background of the beam compression, while for $P < P_{\rm cr}$, the semiaxes oscillate simultaneously with the beam broadening. As an example, Fig. 2 demonstrates for a beam with the initial axial ratio $a/b = 2$ the windows with tinted patterns of the intensity distribution $I(x, y)/I_0$ in the beam cross section at different distances z for the power $P = 2P_{\rm cr}(a/b = 2)$. The scale along the longitudinal coordinate z is the quantity $L_\parallel = kab$, which characterises the linear diffraction of the elliptic beam.*

One can see from Fig. 2 that the beam in which the horizontal size exceeds the vertical one ($z = 0.16L_\parallel$), becomes first close to the circular beam ($z = 0.64L_\parallel$), and then the horizontal size becomes smaller than the vertical one ($z = 0.96L_\parallel$), this process being accompanied by the beam compression as a whole.

The power flux in the in the beam cross section localised at the beam axis is not axially symmetric, and the flux direction in some regions of the beam cross section changes during self-focusing. This is clearly demonstrated by the distribution of the gradient of the light-field phase $\varphi(x, y)$. The plots $(\partial\varphi/\partial x)\mathrm{sign}\,x$ and $(\partial\varphi/\partial y)\,\mathrm{sign}\,y$ of the quantities φ^* determining the direction of the power flux, calculated for $y = 0$ and $x = 0$, are presented at the boundaries of windows in Fig. 2. At the beginning of self-focusing ($z = 0.16L_\parallel$), the power flux in the axial region contains components directed to the beam centre. Outside this region, the power flux along the minor semiaxis, where diffraction is manifested stronger, transfers to the beam periphery. For $z = 0.64L_\parallel$, the diffraction-limited divergence along the vertical semiaxis becomes dominant and the outflow of light-field power from the beam centre occurs. The beam size increases in this direction, and at the distance $z = 0.96L_\parallel$ the vertical semiaxis of the elliptic cross section becomes larger than the horizontal semiaxis. In this case, as follows from analysis, the power transfers in the beam-centre vicinity, where the beam takes the form close to axially symmetric. As z further increases ($z = 1.36L_\parallel$), the power in the axial region contracts to the beam centre along both directions. At the distance $z = 1.76L_\parallel$ the power flux toward the beam centre rapidly increases, by forming a nonlinear focus with the axially symmetric intensity distribution.

Figure 3 shows the dependences of the transverse dimensions of the beam at the e^{-1} level on the distance, which were obtained for different axial ratios a/b of the initially elliptic cross section for the beam power $P = 1.2P_{\rm cr}(a/b)$. One can see that at the same relative excess over the critical power $P_{\rm cr}(a/b)$, the amplitude of oscillations of semiaxis sizes increases with increasing the ratio a/b for the initial elliptic beam. The oscillations of the transverse sizes of the elliptic beam appear due to the competition of the diffraction divergence and nonlinear

* Note that the scale can be chosen arbitrarily, and the diffraction lengths of a circular beam ka^2 and kb^2, the nonlinearity length $n_0/(2kn_2|E_0|^2)$, etc. can be used as the scale.

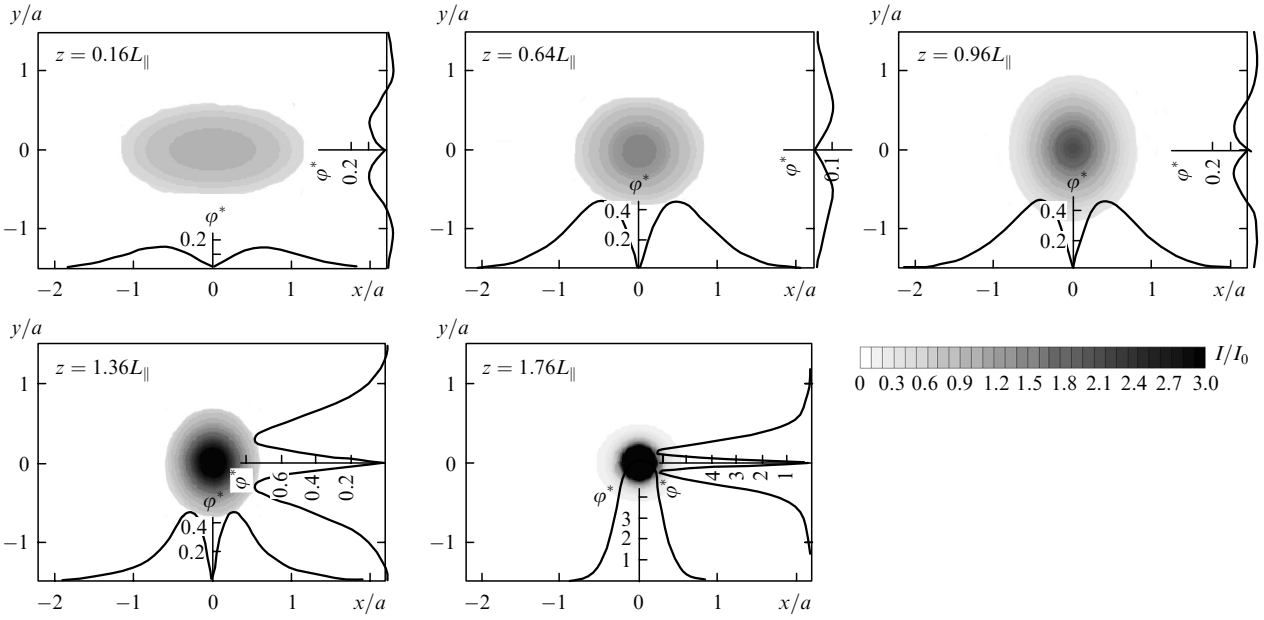

Figure 2. Tinted patterns of the intensity distribution $I(x, y)/I_0$ in the beam cross section (inside windows) and the plots of phase gradients $(\partial\varphi/\partial x)\mathrm{sign}\,x|_{y=0}$ and $(\partial\varphi/\partial y)\mathrm{sign}\,y|_{x=0}$ (at window boundaries) at different distances z in the case of aberration-free self-focusing of the beam with the initial axial ratio $a/b = 2$ and the power $P = 2P_{\rm cr}$. The distance z is presented in the units of the longitudinal scale $L_\parallel = kab$; φ^* is expressed in radians.

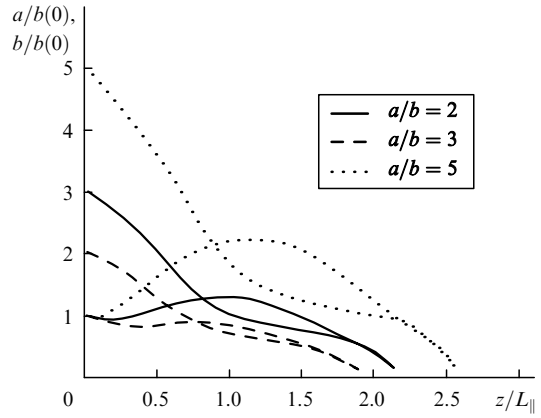

Figure 3. Dependences of the transverse sizes a and b of beam on the distance z for the initial axial ratio equal to $a/b = 2$, 3, and 5 for $P = 1.2P_{cr}(a/b)$.

compression and depend on the axial ratio of the initial cross section of the beam and its power.

5. Aberration self-focusing

The transverse dimensions of the beam determine uniquely its profile under the conditions of aberration-free self-focusing in form (2). At the same time, the transformation of the beam profile depends on its power and ellipticity of the initial intensity distribution. As the power P of the elliptic beam increases, the aberration distortions of its profile appear. Thus, a beam with $a/b = 5$ remains unimodal, but its profile substantially differs from a Gaussian.

For $P = 25P_{cr}$, the power density in the beam cross section is redistributed in a complicated way (Fig. 4). A strong nonlinear compression of the beam along the minor semiaxis, which is ahead of self-focusing in the perpendicular direction, results in the formation of the waist in the beam profile in the elliptic cross section ($z = 0.045L_{\|}$). The power has no time to transfer to the beam centre along the major semiaxis of the cross section, and the beam decomposes due to the diffraction-limited divergence in the transverse direction ($z = 0.06L_{\|}$). As a result, two maxima are formed on the major axis, which grow, drawing out power from the adjacent region. Having achieved the intensity exceeding the initial intensity approximately by an order of magnitude, they cease to grow ($z = 0.07L_{\|}$). Simultaneously, two other maxima begin to form on the minor semiaxis. The power flux directed to these maxima increases their intensity and simultaneously depletes the maxima formed earlier on the major semiaxis ($z = 0.085L_{\|}$). Later, the growing maxima merge into one (central) maximum, around which a complex distribution of the power density without the axial symmetry remains ($z = 0.096L_{\|}$). As z increases, one maximum appears on the beam axis, by forming a nonlinear focus, and a part of the power remains at the beam periphery.

6. Self-focusing distance

Despite the aberration nature of the profile transformation of the initially elliptic beam during self-focusing, one global axially symmetric maximum is formed in which the intensity distribution is close to the Townes mode [18]. Later, a nonlinear focus is formed from this maximum. The numerical study in the approximation of slowly varying amplitudes allows one to estimate the self-focusing length z_f as a distance at which the intensity distribution for the global maximum becomes axially symmetric and its value exceeds the initial value by more than two – three orders of magnitude. The error of this estimate of z_f is small because the intensity in the maximum rapidly increases with approaching the nonlinear focus.

Figure 5 shows the dependences of the self-focusing length z_f of elliptic beams on the power P for different axial ratios a/b of the initial cross section. One can see that the found values of z_f, irrespective of the axial ratio a/b of the initial elliptic cross section and the relative power $P/P_{cr}(a/b)$, belong to one dependence $z_f = z_f(P/P_{cr})$. By using the method of least-squares, we obtained the approximate expression for the dependence of the self-focusing length z_f of the elliptic beam with the axial ratio a/b on its longitudinal scale $L_{\|} = kab$ and the ratio of its power P the critical power $P_{cr}(a/b)$

$$z_f = 0.367L_{\|}\left\{\left[\left(\frac{P}{P_{cr}(a/b)}\right)^{1/2} - 0.852\right]^2 - 0.0219\right\}^{-1/2}. \quad (7)$$

Dependence (7) is the generalisation of the known Marburger formula [11] for circular beams to elliptic beams.

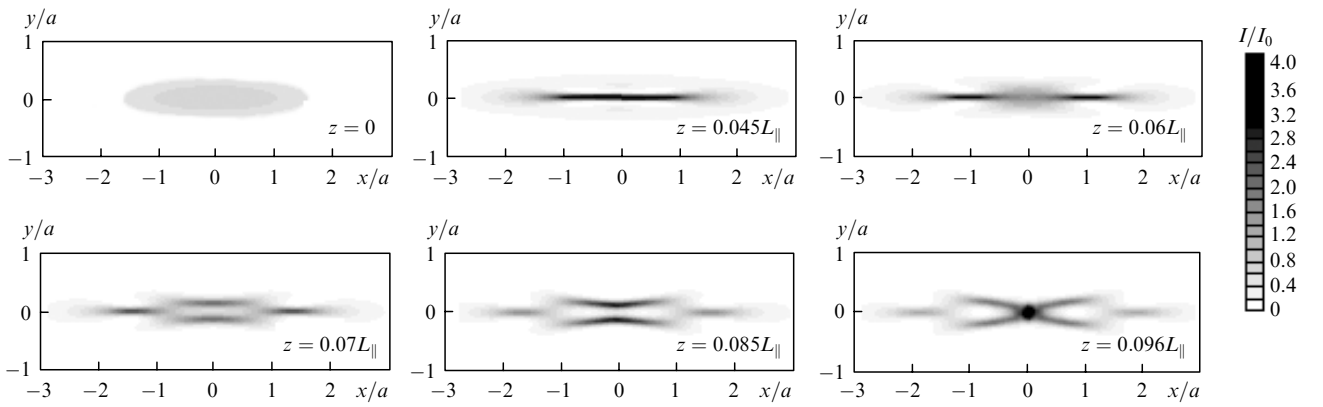

Figure 4. Tinted patterns of the intensity distribution $I(x, y)/I_0$ in the beam cross section at different distances z in the case of aberration self-focusing of the beam with the initial axial ratio $a/b = 5$ and power $P = 25P_{cr}$. The distance z is presented in the units of the longitudinal scale $L_{\|} = kab$.

The longitudinal scale $L_\parallel$ in this formula coincides with the diffraction length $L_\parallel = ka^2$, while the critical power P_{cr} $(a/b = 1)$ is determined by expression (5) with R_{cr} $(a/b = 1) = 3.77$. Note that this dependence is valid both for aberration-free self-focusing of the beam and for self-focusing with strong aberrations. The error of generalised expression (7) over the entire power range and different axial ratios of the elliptic beam considered here does not exceed 10 % for $P \geqslant P_{cr}$ and increases up to 35 % for $P \approx 1.2P_{cr}$.

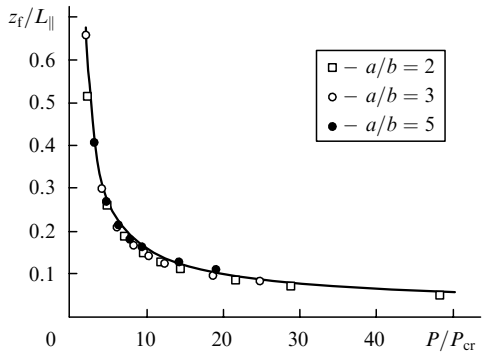

Figure 5. Dependences of the self-focusing length $z_f/L_\parallel$ of the elliptic beam on its relative power P/P_{cr} for different axial ratios a/b; the curve is constructed by approximate expression (7).

7. Conclusions

1. The critical self-focusing power P_{cr} of elliptic beams increases with increasing the axial ratio a/b of the initial intensity distribution in the beam cross section. The variational method with the aberration-free approximation overestimates the critical self-focusing power. The relative deviation of the variational estimate from the result of numerical simulation increases with increasing the axial ratio of the elliptic intensity distribution.

2. The propagation of elliptic beams in a medium with the cubic nonlinearity is accompanied by oscillations of their transverse dimensions, which occur against the background of the diffraction-limited divergence for $P < P_{cr}$ or nonlinear compression for $P > P_{cr}$. The amplitude of oscillations increases with increasing a/b. The oscillations of semiaxes are caused by the competition between diffraction and self-focusing and appear due to transfer of power in the cross section plane, resulting in the formation of a global maximum with profile close to the Townes mode.

3. As the axial ratio a/b of the elliptic cross section and its power P increase, the beam self-focusing acquires the aberration nature. In the beam cross section a competition takes place between the intensity maxima formed, resulting in their mutual suppression, the appearance of new maxima and, finally, the formation of a nonlinear focus at the beam centre.

4. The self-focusing length z_f of the elliptic beam with the axial ratio a/b of the initial intensity distribution depends on its longitudinal scale $L_\parallel = kab$ and the ratio of its power P to the critical self-focusing power P_{cr} of a beam with this ratio a/b, and can be calculated from the approximate formula, which is the generalisation of the expression for circular beams [11] to the case of elliptic beams.

Acknowledgements. This work was supported by the Russian Foundation for Basic Research (Grant No. 03-02-16939), the European Office of Scientific Research of the USA Army (Contract No. N62558-04-P-6051) and the CRDF GAP Grant No. RPO-1390-TO-03).

Appendix

Variational-difference method

Because a nonuniform grid does not allow the use the spectral method with the fast Fourier transform algorithm, we constructed a conservative difference scheme on the nonuniform grid by the variational method [20]. The construction of the variational-difference scheme on a uniform grid and analysis of its accuracy are presented in [21].

The variational-difference scheme was constructed to perform the splitting procedure according to which the solution of Eqn (3) at the integration step Δz along the z axis is replaced by the successive solution of two-dimensional diffraction problems in a linear medium, first in the planes parallel to XZ and then in the planes parallel to YZ. Then, a nonlinear phase shift of the light field is calculated in the same interval Δz in the absence of diffraction.

The solution of the diffraction problem is equivalent to the search for the amplitude $E(x, y, z)$ at which the Lagrangian $L[E, E^*]$ achieves its minimum [22]. In the case of diffraction in the YZ plane in the interval (z_j, z_{j+1}), the Lagrangian has the form [10, 21]

$$L[E, E^*] = \int_{z_j}^{z_{j+1}} \mathrm{d}z \int_{-\infty}^{\infty} \mathrm{d}x \times \left[2\mathrm{i}k \left(\frac{\partial E}{\partial z} E^* - \frac{\partial E^*}{\partial z} E \right) + \frac{\partial E}{\partial x} \frac{\partial E^*}{\partial x} \right]. \quad \text{(A1)}$$

In the variational-difference method, as in the method of finite elements [23], the amplitude $E(x, z)$ minimising the functional $L[E, E^*]$, is represented by a combination of functions defined on the grid meshes. The amplitude $E(x, z)$ in the first term of the integrand in (A1) is assumed constant in grid meshes and equal to the node value $E_m(z)$

$$E(x, z) = E_m(z). \quad \text{(A2)}$$

The amplitude $E(x, z)$ in the second term in (A1) changes linearly between the grid nodes:

$$E(x, z) = (E_{m+1}(z)) - E_m(z) \frac{x - x_m}{h_{m+1}} + E_m(z), \quad \text{(A3)}$$

$$x \in [x_m, x_{m+1}],$$

where x_m is the coordinate of the mth node. By substituting (A2) and (A3) into (A1), we perform the approximation of the same order in the coordinate x for all the terms of the Lagrangian. After the replacement of the right-hand in (A1) by a sum of integrals over the regions of definition of the amplitude $E(x, z)$ on the calculation grid, the functional is expressed by the bilinear form $L[E_m, E_m^*]$ with respect to the values E_m and E_m^* in the grid nodes. The minimisation conditions for the functional $\delta L_{E_m^*}[E_m, E_m^*] = 0$ in the set $\{E_m^*, m = -N/2, \ldots, 0, \ldots, N/2\}$ gives the system of difference-differential equations for the complex field amplitude $E_m(z)$

$$2ik\,\frac{h_{m+1}+h_m}{2}\,\frac{\partial E_m(z)}{\partial z}=\frac{E_{m+1}(z)}{h_{m+1}}-\left(\frac{1}{h_{m+1}}+\frac{1}{h_m}\right)E_m(z)$$

$$+\frac{E_{m-1}(z)}{h_m},\qquad z\in[z_s,z_{s+1}]. \tag{A4}$$

At the calculation grid boundary $m=-N/2$, $N/2$, the field amplitudes $E_{-N/2}$ and $E_{N/2}$ are assumed zero. The difference-differential equations for the diffraction problem in planes parallel to the YZ plane are written similarly.

The difference-differential equations of diffraction were integrated with respect to the variable z in the interval (z_s, z_{s+1}) in planes parallel to the XZ and YZ planes by the Crank–Nicholson method [20]. The nonlinear phase shift in the interval (z_s, z_{s+1}) was calculated in the fixed-intensity approximation. The integration step Δz is $0.01kab$ at the beginning of propagation and then it decreased adaptively by half if the maximum nonlinear phase shift exceeds $\pi/100$ in a step $\Delta z=z_{s+1}-z_s$. For the power $P\sim 24P_{cr}$, the integration step in z decreases by a factor of 2^4 at the end of propagation. The beam self-focusing was simulated numerically to the z_s plane where the maximum intensity in the beam cross section exceeded the initial peak intensity I_0 by two orders of magnitude. The calculation region in the XY plane has the form of a square with the side $8a$.

The accuracy of the numerical simulation of self-focusing is controlled by the deviation of the motion integrals – the power P and Hamiltonian H of the light beam. For $P>P_{cr}$, the relative deviation $\Delta P/P$ does not exceed 0.05 % over the entire range of the parameters, while for $P>2P_{cr}$, the relative deviation of the Hamiltonian $\Delta H/H$ is 1 %–2 %. As the beam power decreases down to $P=(1.2-2)P_{cr}$, the absolute value of the Hamiltonian $|H|$ decreases and its relative deviation in calculations increases up to 15 %. For $P\sim P_{cr}$, the beam slowly contracts or diverges with distance, resulting in the accumulation of the calculation error.

The use of the nonuniform grid allows the reduction of the dimensionality of the data arrays being processed and, hence, of the computation time. The analysis of computational schemes on grids with the axial region with a step changing uniformly from $0.25a$ to $1.5a$, of the step value $h_0(0.005a-0.1a)$ and the parameter of its increase ε (0.005–0.1) showed that the minimal computational time is achieved without a substantial loss of accuracy for $h_0=0.01a$, $\varepsilon=0.01$, and the uniform step region equal to $1a$. In this case, the deviation of the Hamiltonian from the values obtained in test calculations on a uniform grid of high dimensionality (1000×1000) did not exceed 1 %. Our estimates showed that for these parameters of the calculation grid the dimensionality of calculation data arrays is reduced by a factor of four and more compared to conventional uniform grids.

References

1. Kasparian J., Rodriguez M., Méjean G., Yu J., Salmon E., Wille H., Bourayou R., Frey S., André Y.-B., Mysyrowicz A., Sauerbrey R., Wolf J. P., Wöste L. *Science*, **301**, 61 (2003).
2. Bergé L., Skupin S., Lederer F., Méjean G., Yu J., Kasparian J., Salmon E., Wolf J. P., Rodriguez M., Wöste L., Bourayou R., Sauerbrey R. *Phys. Rev. Lett.*, **92**, 225002 (2004).
3. Kandidov V.P., Kosareva O.G., Mozhaev E.I., Tamarov M.P. *Opt. Atmos. Okean.*, **13**, 429 (2000).
4. Nibberling E.T.J., Curleg P.F., Grillon G., Prade B.S., Franco M.A., Salin F., Mysyrowicz A. *Opt. Lett.*, **21**, 62 (1996).
5. Kandidov V.P., Kosareva O.G., Golubtsov I.S., Liu W., Becker A., Akozbek N., Bowden C.M., Chin S.L. *Appl. Phys. B*, **77**, 149 (2003).
6. Kasparian J., Sauerbrey R., Chin S. L. *Appl. Phys. B*, **71**, 877 (2000).
7. Rairoux P., Schillinger H., Niedermeier S., Rodriguez M., Ronneberger F., Sauerbrey R., Stein B., Waite D., Wedekind C., Wille H., Wöste L., Ziener C. *Appl. Phys. B*, **71**, 573 (2000).
8. Bespalov V.I., Litvak A.G., Talanov V.I., in *Nelineinaya optika* (Nonlinear Optics) (Novosibirsk: Nauka, 1968) pp 428–463.
9. Liu W., Hosseini S.A., Luo Q., Ferland B., Chin S.L., Kosareva O.G., Panov N. A., Kandidov V.P. *New J. Phys.*, **6**, 6 (2004).
10. Vorob'ev V.V. *Izv. Vyssh. Uchebn. Zaved., Ser. Radiofiz.*, **13**, 1905 (1970).
11. Marburger J.H., in *Prog. Quantum Electron.* (Great Britain: Pergamon Press, 1975) Vol. 4, p. 35.
12. Egorov K.D., Kandidov V.P. *Vestn. Mosk. Univ., Ser. Fiz. Astron.*, **19**, 70 (1978).
13. Cornolty F., Lucchesi M., Zambon B. *Opt. Commun.*, **15**, 129 (1990).
14. Akhmanov S.A., Sukhorukov A.P., Khokhlov R.V. *Usp. Fiz. Nauk*, **93**, 19 (1967).
15. Tarsem Singh, Nareshpal Saini, Shyam Sunder Kaul *Pramana J. Phys.*, **55**, 423 (2000).
16. Gross B., Manassah J.T. *Phys. Lett. A*, **169**, 371 (1992).
17. Fibich G., Ilan B. *Opt. Soc. Am. B*, **17**, 1749 (1999).
18. Chiao R., Garmire E., Townes C. *Phys. Rev. Lett.*, **13**, 479 (1964).
19. Fibich G., Gaeta A.L. *Opt. Lett.*, **25**, 335 (2000).
20. Kalitkin N.N. *Chislennye metody* (Numerical Methods) (Moscow: Nauka, 1978).
21. Egorov K.D., Kandidov V.P., Ledenev V.I. *Zh. Vycisl. Mat. Mat. Fiz.*, **22**, 382 (1982).
22. Mikhlin S.G. *Variatsionnye metody v matematicheskoi fizike* (Variational Methods in Mathematical Physics) (Moscow: Nauka, 1970).
23. Zenkevich O. *Metod konechnykh elementov v tekhnike* (Method of Finite Elements in Technique (Moscow: Mir, 1975).